Laser cooling in an optical lattice that employs Raman transitions

R. Zhang, N. V. Morrow, P. R. Berman, and G. Raithel
FOCUS Center, Michigan Center for Theoretical Physics, and Department of Physics, University of Michigan, Ann Arbor, Michigan 48109, USA
(Received 7 April 2005; published 28 October 2005)

We demonstrate laser cooling in an optical lattice that employs Raman transitions. Four laser beams with different frequencies form a one-dimensional lattice with a basic lattice period that is a factor of 2 less than in standard optical lattices. Rb atoms are cooled to 8 μK. We measure the intensity- and detuning-dependence of the cooling mechanism. Our experimental results agree well with theoretical models.

DOI: 10.1103/PhysRevA.72.043409 PACS number(s): 32.80.Pj, 33.80.Wz

An optical lattice is a periodic light-shift potential created by the interference of several laser beams [1]. Different methods can be used to localize cold atoms at the minima of these potentials. The most straightforward one is to employ lattice parameters that lead to Sisyphus cooling [2]. Optical lattices have found an array of applications in current research, from studies of basic quantum mechanical phenomena [3] to quantum computing schemes [4]. Due to their naturally periodic structure that is inherently defect-free, they also are finding use in applied fields such as nanolithography [5].

The basic periodicity of an optical lattice produced by a laser field having wavelength λ is $\lambda/2$, although structures as small as $\lambda/8$ [6] can be created in certain cases. In a number of papers it has been demonstrated that it is possible to reduce this basic periodicity by a factor of 2 or more [7–10] by modifying the atom-field geometry. Moreover, it has been proposed recently [11] that sub-Doppler cooling occurs for one such scheme that we refer to as a Raman optical lattice (ROL). In this paper, we provide experimental proof of sub-Doppler laser cooling in the ROL scheme, and we measure its dependence on laser frequency and intensity. The one-dimensional ROL utilizes Raman transitions between two ground-state magnetic sublevels, leading to a reduction of the lattice period by a factor of 2. Monte Carlo simulations reproduce the experimentally observed cooling behavior of the ROL very well, providing indirect evidence for its reduced periodicity.

The energy level diagram and field directions and polarizations are shown in Fig. 1. The ROL is created by two pairs of counterpropagating laser fields. Due to their polarizations, fields 1, 4 drive only $|m=-1\rangle \rightarrow |e\rangle$ transitions and fields 2, 3 drive only $|m=1\rangle \rightarrow |e\rangle$ transitions. The atom-field detunings Δ_1, Δ_2 (typically 20 MHz or so) are sufficiently large to ensure that the excited state is never significantly populated. A homogeneous magnetic field provides a frequency separation of the $|m=-1\rangle$ and $|m=1\rangle$ magnetic sublevels that are in the range ±200 kHz.

We first consider the pair of fields 1 and 3 in Fig. 1, which have propagation vectors $\mathbf{k}_1=-\mathbf{k}_3=\mathbf{k}=(2\pi/\lambda)\hat{\mathbf{z}}$. An atom initially in $|m=-1\rangle$ can absorb one photon from field 1, reemit a photon into field 3, and end up in state $|m=1\rangle$. In this process, the atom receives a momentum kick equal to $2\hbar\mathbf{k}$. Thus the $|m=-1\rangle$ and $|m=1\rangle$ magnetic sublevels are coupled by a two-photon process that is driven by an effective Raman field with a propagation vector $2\mathbf{k}$. The fields 2 and 4 couple the magnetic sublevels in a similar manner but have directions opposite to those of fields 1 and 3. Thus beams 2 and 4 are equivalent to a Raman field with propagation vector $-2\mathbf{k}$. The two counterpropagating Raman fields interfere in driving transitions between the two magnetic sublevels $|m=-1\rangle$ and $|m=1\rangle$. To lowest order in the Raman field strength, this leads to a modulation of ground state population difference and coherence that varies as $\cos(4kz)$. In this manner, a density grating having period $\lambda/4$ can be created. The physical origin of the sub-Doppler friction force differs from that of conventional sub-Doppler "corkscrew" cooling [2,11]. Had we considered the effect of only a single pair of Raman fields (e.g., 1 and 3) as in a gray optical lattice, the friction force would vanish for our Λ-type level scheme, resulting from an *exact cancellation* of contributions arising from a motionally induced imbalance in ground state populations [2] and a spatially modulated phase associated with the ground state sublevel coherence [12]. In the ROL, the combined action of all fields leads to a friction force that arises mainly from the spatially modulated ground state coherence—for two photon resonance, there is no population imbalance of the $|m=-1\rangle$ and $|m=1\rangle$ states [11].

A frequency difference $\Delta_{21}=\Delta_2-\Delta_1$ of a few MHz between fields 1 and 4 and fields 2 and 3 is introduced. As long as $|\Delta_{21}|$ is much greater than the effective two-photon Rabi frequency coupling between the $|m=-1\rangle$ and $|m=1\rangle$ states, one suppresses interactions in which fields 1 and 2 (or 4 and 3) drive such transitions and allows one to neglect modulated Stark shifts of the levels produced by fields 1 and 4 (or 2 and 3) [11].

In the experiment, ^{87}Rb atoms are first cooled and col-

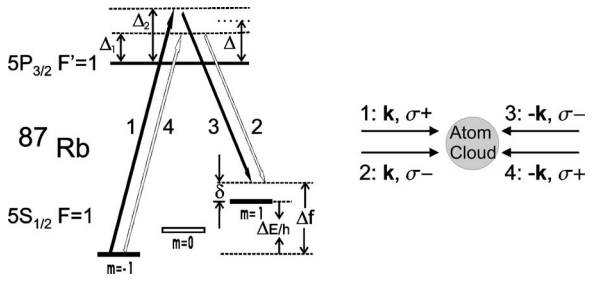

FIG. 1. Level scheme and field directions and polarizations.

lected in a vapor-cell magneto-optic trap (MOT) and further cooled for 1 ms in an optical molasses to ~50 μK. The Raman lattice is then applied for durations ranging from a few to 150 μs. In our demonstration, we have implemented an atom-field detuning difference of $\Delta_2-\Delta_1=4$ MHz. The average atom-field detuning $\Delta=(\Delta_1+\Delta_2)/2$ can be set between -15Γ and $+16\Gamma$ relative to the 780 nm, $5S_{1/2}$, $F=1\rightarrow 5P_{3/2}$ $F'=1$ transition ($\Gamma=6$ MHz is the excited state decay rate divided by 2π). In order to optically pump the atoms into the active $F=1$ state of the ROL, a repumper beam that is on-resonance with the $5S_{1/2}$ $F=2\rightarrow 5P_{3/2}$ $F'=2$ transition is applied during the ROL phase. In the presently investigated scheme, both Raman transitions of the ROL scheme possess the same Raman detuning δ. The value of δ is determined by both the frequency difference between the Raman beams, labeled Δf in Fig. 1, and the energy separation between the $|m=-1\rangle$ and $|m=1\rangle$ states, which is tuned by a magnetic field parallel to the lattice-beam direction.

All four ROL beams are derived from a single, frequency-stabilized diode laser. The output beam is split into four beams, which are then frequency-shifted by individual amounts using acousto-optic modulators (AOMs). The AOMs are driven by four rf signals generated by rf signal sources and a custom rf circuit built from standard parts (IQ modulators, 0° and 180° power splitters, amplifiers). In this scheme, the frequency *differences* of the four ROL beams are very stable, as required for the ROL. The frequency fluctuations of the laser are much less than Γ and affect all ROL beams equally, and therefore do not significantly affect the ROL performance.

Spatial mode-matching of copropagating pairs of beams (1 with 2 and 3 with 4) is achieved by coupling each beam pair into two orthogonal modes of a shared polarization-maintaining optical fiber using polarization optics. The combined beams coupled out of the fibers are passed through $\lambda/4$ wave plates, leading to the polarizations indicated in Fig. 1, and are directed vertically from opposite directions into the chamber. The spatial profiles of the beams at the location of the atomic cloud are approximately Gaussian with a FWHM diameter of 8 mm.

The temperatures obtained in the ROL are measured using the standard time-of-flight (TOF) method [13,14]. The TOF probing beam is a cylindrically collimated sheet of on-resonant light ~0.4 mm thick, located 20 cm below the MOT position. As the atoms fall through the TOF probe beam, their fluorescence is detected by a large-area photodiode. The momentum distribution of the atoms follows from the time dependence of the fluorescence signal.

In Fig. 2(a) we compare typical momentum distributions (in units of recoil momentum $p_{\mathrm{rec}}=\hbar k$) measured after cooling in a standard six-beam optical molasses and after additional cooling in the ROL ($\delta=0$, $\Delta=3\Gamma$, 1 mW/cm^2 single-beam intensity, 150 μs lattice time). Fitting the data with Gaussians, we find that the typical molasses temperature is 50 μK, while the ROL cools the atoms further to 8 μK. The presence of sub-Doppler cooling in the ROL is therefore established.

To characterize the speed of the cooling process, we have varied the duration of ROL cooling in steps of 10 μs. The resultant momentum distributions are assembled in a two-dimensional (2D) data set, which is displayed in Fig. 2(b). For the lattice parameters of Fig. 2 it is found that steady state is achieved in about 70 μs.

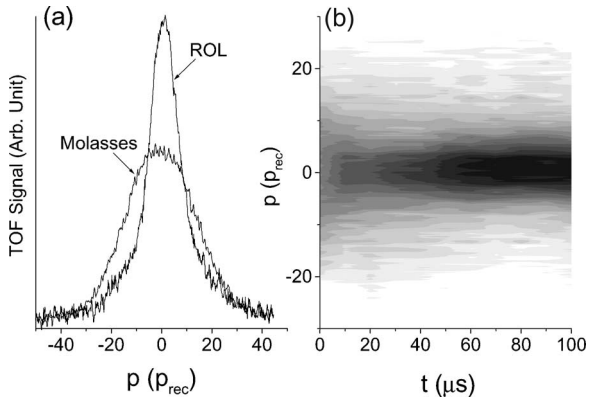

FIG. 2. (a) Momentum distributions of atoms cooled by optical molasses and by ROL, respectively. (b) 2D plot of momentum distribution of atoms vs cooling time in ROL.

An important characteristics of laser cooling is the dependence of the steady-state temperature on the intensity of the laser beams. We have measured steady-state momentum distributions as a function of the single-beam intensity I at the center of the lattice beams and fitted them with Gaussians. The resultant standard deviations σ_p yield temperatures $T=\sigma_p^2/Mk_B$, where M is the atomic mass and k_B the Boltzmann constant, which are shown by the circles in Fig. 3. We have compared the experimental results with quantum Monte Carlo wave-function simulations (QMCWF) [11]. The simulations describe the center-of-mass motion of the atoms trapped in the ROL in a fully quantum-mechanical way for the exact atomic parameters and laser-beam characteristics used in the experiment. The squares in Fig. 3 show temperatures obtained from Gaussian fits to the simulated momentum distributions. Both in theory and experiment, we observe a linear relationship between intensity and temperature, and experimental and theoretical results agree to within 20%. The discrepancy may be caused by the Gaussian intensity profile of the laser beams, due to which the average intensity experienced by the atoms is slightly below the intensity I at

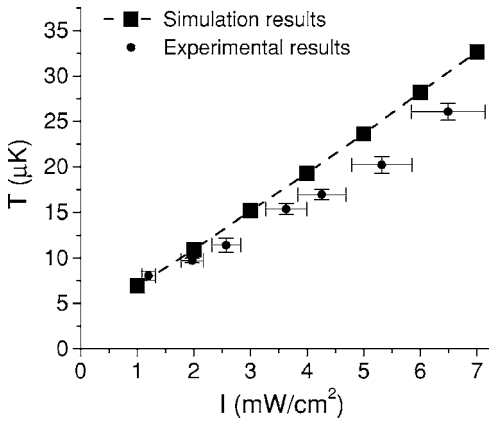

FIG. 3. Intensity dependence of ROL cooling. Circles show experimental results and squares results of QMCWF simulations.

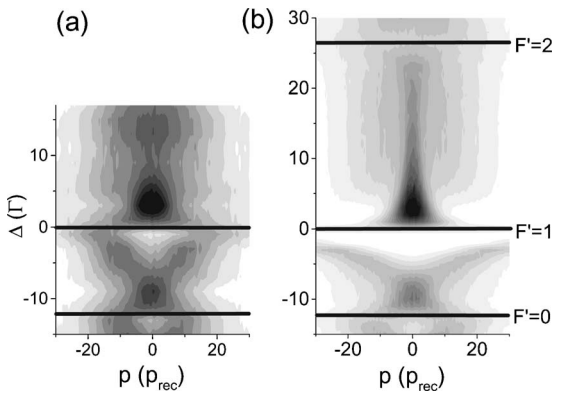

FIG. 4. (a) 2D plot of momentum distributions of atoms for different atom-field detunings Δ. (b) Simulation results.

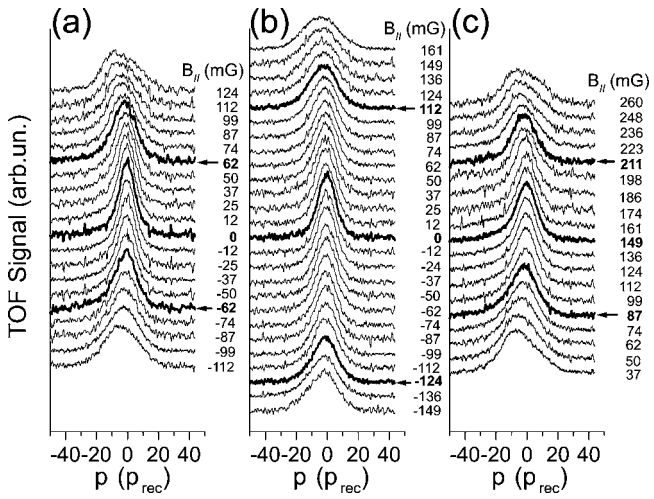

FIG. 5. (a) Momentum distributions of atoms in ROL for the indicated longitudinal magnetic fields and $\Delta f = f_1 - f_3 = 0$. Single-beam intensity is 1 mW/cm^2. (b) Same as (a) except that single-beam intensity is 2 mW/cm^2. (c) A 200 kHz frequency difference $\Delta f = -200$ kHz is applied. Single beam intensity is 1 mW/cm^2. The arrows indicate the boundaries of the cooling ranges defined in the text (1 mG corresponds to a change of 1.4 kHz in the detuning δ).

the beam center. The QMCWF also reproduce the time dependence of laser cooling in the ROL, shown in Fig. 2(b), in a satisfactory manner.

As in standard optical lattices, where the detuning of the laser frequency greatly affects the Sisyphus cooling [1], in the ROL the atom-field detuning Δ is also very important. In Fig. 4(a) we show experimental momentum distributions as a function of atom-field detuning Δ relative to the $F=1 \rightarrow F'=1$ transition varied in steps of 2Γ, while Fig. 4(b) offers corresponding results of QMCWF simulations. The latter extend beyond the $F'=2$ level (this was not possible experimentally due to technical reasons). Experimental and theoretical results generally agree well. Cooling occurs when the laser fields are slightly blue-detuned relative to the $F=1 \rightarrow F'=0$ and $F=1 \rightarrow F'=1$ transitions, and clearly works best for the $F=1 \rightarrow F'=1$ transition. No cooling is observed for either blue- or red-detuning from the $F=1 \rightarrow F'=2$ transition.

The detuning-dependence observed in the vicinity of the $F=1 \rightarrow F'=0$ and $F=1 \rightarrow F'=1$ transitions can be qualitatively explained using a result of the semiclassical treatment of the ROL in Ref. [11]. There, the spatially averaged friction force on the atoms for $|\Delta| > \Gamma$ is found to be

$$\bar{F} \approx -\frac{2\chi^2}{\Delta}\hbar k \frac{\alpha}{1+\alpha^2}, \tag{1}$$

where $\alpha \approx \Delta^2 kv/\chi^2\Gamma$ and χ is the Rabi frequency and v is the velocity of the atoms. For positive Δ (blue-detuning), the friction force opposes the direction of motion, leading to sub-Doppler cooling. At small velocities, α in Eq. (1) is less than 1, and the friction force tends to be $\propto v\Delta$. Thus lower temperatures should be achieved at larger detunings. In Fig. 4, this trend is generally observed for blue-detunings less than $\sim 5\Gamma$ relative to the $F=1 \rightarrow F'=0$ and $F=1 \rightarrow F'=1$ transitions. Since the velocity capture range v_c of the friction force, identified by $[d\bar{F}/dv]\,(v_c)=0$, decreases as $\propto \chi^2/\Delta^2$, the cooling becomes ineffective for larger blue-detunings. For negative Δ (red-detuning), the friction force and v have the same sign. Thus atoms will accelerate away from $v=0$ ("sub-Doppler heating"). The acceleration eventually diminishes, as α increases with v. The net effect is that atoms should emerge with a (nonstationary) two-peak momentum distribution, as observed in Fig. 4 for red-detunings less than $\sim 5\Gamma$ relative to the $F=1 \rightarrow F'=0$ and $F=1 \rightarrow F'=1$ transitions. We have verified that the double-peaked momentum distributions are nonstationary; the separation between the two peaks gradually increases as a function of heating time in the ROL. Furthermore, for large v, α is much larger than 1. Under this condition, the heating force $\bar{F} \propto v\Delta^{-3}$. This explains why the separation between the two peaks is larger for smaller Δ. In a quantitative analysis, momentum diffusion must be considered in addition to friction [11].

To understand the qualitative differences in behavior in the vicinity of different upper-state hyperfine levels F', we need to take into account the magnetic sublevel $|m=0\rangle$ that is not directly coupled by the fields (see Fig. 1). Near the $F=1 \rightarrow F'=0$ transition, atoms falling into that state require a long time to be optically pumped back into one of the active $|F=1, m=\pm 1\rangle$ states through off-resonant excitation into $|F'=1, m'=\pm 1\rangle$ and subsequent decay into $|F=1, m=\pm 1\rangle$. The long dwell time of atoms in the inactive state reduces the ROL cooling and heating efficiency. In contrast, near the $F=1 \rightarrow F'=1$ transition the σ-polarized lattice beams rapidly repump atoms out of the $|m=0\rangle$ state into one of the active levels. Thus cooling and heating processes are expected to be more efficient near the $F=1 \rightarrow F'=1$ transition, as observed. Finally, the heating effect associated with near-resonant excitation from $|F=1, m=\pm 1\rangle$ into $|F'=2, m'=\pm 2\rangle$ entirely disables the ROL close to the $F=1 \rightarrow F'=2$ transition frequency, as is evident in Fig. 4.

We also study how the ROL cooling depends on δ. In our experiment, $\delta = \Delta f - \Delta E/h$, where $\Delta f = f_1 - f_3 = f_4 - f_2$ is the frequency difference between the beams driving the Raman transitions, and $\Delta E = -\mu_B B$ is the Zeeman splitting between $|m=1\rangle$ and $|m=-1\rangle$ due to a longitudinal magnetic field B [see Fig. 1]. Thus δ can be varied by both Δf and B. We keep the frequency difference Δf fixed and take the TOF signals

as a function of B, which is varied in steps of 12.4 mG, equivalent to steps of 17.4 kHz in δ. Figures 5(a) and 5(b) show the measured momentum distributions for $\Delta f=0$ for single-beam intensities of 1 and 2 mW/cm^2, respectively. In both cases, we observe cooling over a certain range of B, and the cooling is symmetric about $B=0$. Defining the cooling range $-\delta_c<\delta<\delta_c$ as the range of δ over which the temperature is less than twice the temperature at $\delta=0$, we obtain $\delta_c=85$ and 160 kHz for Figs. 5(a) and 5(b), respectively. This result suggests that the cooling range is proportional to intensity. In Fig. 5(c) we apply a frequency difference $\Delta f=-200$ kHz. The cooling range is found to remain almost the same as for $\Delta f=0$, whereby best cooling occurs at $B=150$ mG. At this field value, $\delta\approx 0$, i.e., the Zeeman shift cancels the applied frequency difference Δf. Thus laser cooling in the ROL performs best for zero two-photon detuning δ. This is in contrast to conventional Sisyphus cooling, where a nonzero single-photon detuning is required to avoid excessive light scattering. This contrast in detuning behavior reflects the fact that the two cooling mechanisms are qualitatively different. QMCWF simulations are in good agreement with the observations in Fig. 5. Detailed theoretical results for $\delta\neq 0$ will appear elsewhere.

Besides sub-Doppler cooling, another important property of the ROL is the modulation depth of the steady-state atomic density distribution. Presently, we rely on QMCWF results to estimate the density modulation depth. As expected, we find that the modulation period is $\lambda/4$, and that the density distributions of atoms in the $|m=\pm 1\rangle$ states are identical. For $\Delta=3\Gamma$, the modulation depth, defined as the difference between highest and lowest density divided by their sum, ranges from 0.13 to 0.25, as the single-beam intensity I is varied from 1 to 7 mW/cm^2.

In summary, we have shown that Raman optical lattices are suited to laser-cool atoms to temperatures below 10 μK. We have studied the dependence of the cooling on intensity and detuning. Experimental results are in good agreement with theory. Raman lattices may have atom-lithographic applications that call for reduced-period structures. Moreover, they offer the opportunity for increasing the density and interatomic interactions in BECs in situations where there is one atom per lattice site. In future work we plan to verify experimentally the $\lambda/4$ periodicity of the ROL using optical-mask techniques [15] and Bragg scattering methods [16]. An extension of the ROL scheme to higher-order Raman transitions, which are expected to yield even lower lattice periods, will also be pursued.

This research has been supported by National Science Foundation under Grants No. PHY-0244841 and No. PHY-0245532, and FOCUS (PHY-0114336).

[1] P. S. Jessen and I. H. Deutsch, Adv. At., Mol., Opt. Phys. **37**, 95 (1996), and references therein.

[2] J. Dalibard and C. Cohen-Tannoudji, J. Opt. Soc. Am. B **11**, 2023 (1989); P. Verkerk, B. Lounis, C. Salomon, C. Cohen-Tannoudji, J. Y. Courtois, and J. Grynberg, Phys. Rev. Lett. **68**, 3861 (1992); P. S. Jessen, C. Gerz, P. D. Lett, W. D. Phillips, S. L. Rolston, R. J. C. Spreeuw, and C. I. Westbrook, *ibid.* **69**, 49 (1992).

[3] B. P. Anderson and M. A. Kasevich, Science **282**, 1686 (1998); S. K. Dutta, B. K. Teo, and G. Raithel, Phys. Rev. Lett. **83**, 1934 (1999); M. Greiner *et al.*, Nature (London) **415**, 39 (2002).

[4] C. Monroe, Nature (London) **416**, 238 (2002).

[5] G. Grynberg and C. Robilliard, Phys. Rep. **355**, 335 (2001), and references therein.

[6] R. Gupta, J. J. Mc Clelland, P. Marte, and R. J. Celotta, Phys. Rev. Lett. **76**, 4689 (1996).

[7] P. R. Berman, B. Dubetsky, and J. L. Cohen, Phys. Rev. A **58**, 4801 (1998).

[8] B. Dubetsky and P. R. Berman, Laser Phys. **12**, 1161 (2002).

[9] B. Dubetsky and P. R. Berman, Phys. Rev. A **66**, 045402 (2002).

[10] M. Weitz, G. Cennini, G. Ritt, and C. Geckeler, Phys. Rev. A **70**, 043414 (2004).

[11] P. R. Berman, G. Raithel, R. Zhang, and V. S. Malinovsky Phys. Rev. A **72**, 033415 (2005).

[12] C. Cohen-Tannoudji, in *Laser Manipulation of Atoms and Ions*, Course CXVIII of International School of Physics "Enrico Fermi," edited by E. Arimondo, W. D. Phillips, and F. Strumia (North Holland, Amsterdam, 1992) pp. 99–169. See Eq. (4.31).

[13] P. D. Lett, R. N. Watts, C. I. Westbrook, W. D. Phillips, P. L. Gould, and H. J. Metcalf, Phys. Rev. Lett. **61**, 169 (1988).

[14] S. K. Dutta, N. V. Morrow, and G. Raithel, Phys. Rev. A **62**, 035401 (2000).

[15] A. Turlapov, A. Tonyushkin, and T. Sleator, Phys. Rev. A **68**, 023408 (2003).

[16] G. Birkl, M. Gatzke, I. H. Deutsch, S. L. Rolston, and W. D. Phillips, Phys. Rev. Lett. **75**, 2823 (1995); G. Raithel, G. Birkl, A. Kastberg, W. D. Phillips, and S. L. Rolston, *ibid.* **78**, 630 (1997); A. Görlitz, M. Weidemuller, T. W. Hansch, and A. Hemmerich, *ibid.* **78**, 2096 (1997).